

EVOLUTION OF ISOLATED HALOS AND HALOS INSIDE OF GROUPS AND CLUSTERS IN A Λ CDM MODEL

S. Gottlöber^{1,2}, A.A. Klypin², A.V. Kravtsov²

¹*AIP, An der Sternwarte 16, D-14482 Potsdam*

²*Astronomy Department, NMSU, Dept. 4500, Las Cruces, NM 88003-0001*

ABSTRACT. A significant fraction of mass in the universe is believed to be in the form of dark matter (DM). Due to gravitational instability, the DM collapses hierarchically into DM *halos*. In this contribution we present a study of the formation and evolution of such DM halos in a *COBE*-normalized spatially flat Λ CDM model ($\Omega_0 = 1 - \Omega_\Lambda = 0.3$; $h = 0.7$) using high-resolution N -body simulations. The novelty of this study is use of the newly developed halo-finding algorithms to study the evolution of both *isolated* and *satellite* (located inside virial radii of larger group- and cluster-size systems) halos. The force and mass resolution required for a simulated halo to survive in the high-density environments typical of groups and clusters is high: $\sim 1 - 3$ kpc and $\sim 10^9 M_\odot$, respectively. We use the high-resolution Adaptive Refinement Tree (ART) N -body code to follow the evolution of 256^3 dark matter particles with dynamic range in spatial resolution of 32,000 in a box of $60h^{-1}$ Mpc. We show that the correlation function of these halos is anti-biased with respect to the dark matter correlation function and is high and steeper than the correlation function of the isolated virialized objects. The correlation function evolves only mildly between $z = 3$ and $z = 1$. The mass evolution of isolated virialized objects determined from the simulation is in good agreement with prediction of semi-analytical models. The differences exist, however, if we include satellite halos in the halo catalogs.

1 Introduction

It is generally believed that dark matter (DM) constitutes a large fraction of the mass in the Universe. Therefore, it significantly affects both the process of galaxy formation and the large-scale distribution of galaxies. The most convincing observational evidence for substantial amounts of dark matter even in the very inner regions of galaxies comes from recent HI studies of dwarf and low surface brightness galaxies. The gravitational domination of DM on the scale of galaxy virial radius implies that collisionless simulations can be used to study formation of the DM component of galaxies.

A well known problem of dissipationless simulations is overmerging, i.e. the lack of substructure in virialized objects that could be associated with galaxy locations. This effect is due mainly to insufficient force and mass resolution (Moore et

al. 1996; Klypin et al. 1998, hereafter KGKK). Recently, the dynamic range of the N -body simulations has become sufficiently high to overcome this problem. With sufficient resolution the DM halos survive and can be identified in high-density regions even in collisionless simulations (KGKK; Ghigna et al. 1998). This allows us to study halo dynamics and the physical effects of tidal stripping and dynamical friction in group- and cluster-size objects.

In this contribution, we discuss the evolution of DM halos in a spatially flat cosmological model dominated by cold dark matter and non-zero cosmological constant (Λ CDM). Specifically, we study the differences between isolated and satellite halos in their mass evolution and spatial distribution. Scenarios with a Λ -term have become very successful in describing most aspects of cosmological structure formation. We have chosen the following parameters in order to reconcile the model with both

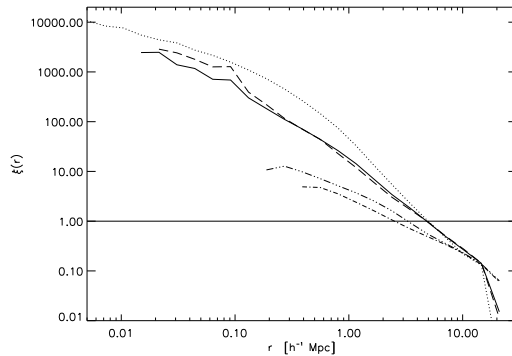


Figure 1. The correlation function of halos with circular velocities $v_{\text{circ}} > 120$ km/s (solid line) and $v_{\text{circ}} > 150$ km/s (dashed line) in comparison to the correlation function of dark matter particles (dotted line). The dashed-dotted lines represent the correlation function of objects found by the friends-of-friends algorithm with the linking radius corresponding to the virial overdensity (dash-dotted for objects with $N > 100$ particles and dash-triple-dotted for $N > 20$).

the COBE measurements and cluster abundance: $\Omega_0 = 1 - \Omega_\Lambda = 0.3$; $h = 0.7$; $\sigma_8 = 1.0$. The age of the universe in this model is ≈ 13.5 Gyrs.

2 Numerical Simulation

In order to study the properties of halos in a cosmological environment, the simulation box should be sufficiently large. On the other hand, to assure that halos do survive also in clusters, the force resolution should be $\sim 1 - 3h^{-1}\text{kpc}$ and the mass resolution should be $\lesssim 10^9 h^{-1}M_\odot$ (Moore et al. 1996; KGKK). The Adaptive Refinement Tree (ART) N -body code (Kravtsov, Klypin & Khokhlov 1997) reaches a formal dynamical range of 32,000 in high density regions, which for the $60 h^{-1}$ Mpc box corresponds to the required necessary force resolution. In the $60 h^{-1}$ Mpc box with 256^3 particles, each particles has a mass of $1.1 \times 10^9 h^{-1}M_\odot$.

Identification of halos in dense environments and reconstruction of their evolution is a challenge. Most widely used halo-finding algorithms, the friends-of-friends (FOF) and the spherical overdensity, both discard “halos inside halos”, i.e. satellite halos located within virial radius of larger halos. The distribution of halos identified in this way, cannot be

compared easily to the distribution of galaxies, because the latter are found within larger systems. In order to cure this, we have developed two related algorithms, which we have called *hierarchical friends-of-friends* (HFOF) and *bound density maxima* (BDM) algorithms (KGKK). These algorithms are complementary. Both find essentially the same halos. The advantage of the HFOF algorithm is that it can handle halos of arbitrary (not only spherically symmetric) shape. The advantage of the BDM algorithm is that it separates background unbound particles from the particles gravitationally bound to the halo, and thus allows a better determination of physical properties of halos.

Since the algorithms work on a snapshot of the particle distribution, they tend to identify also small fake “halos” consisting of only a few *unbound* particles, clumped together by chance at the analyzed moment. We deal with this problem by both checking whether the identified clump is gravitationally bound and by following the merging history of halos. Halos that do not have a progenitor at a previous moment are discarded. For other halos we find the direct progenitor, i.e. a halo at a previous moment that contains the maximum number of particles of this halo. We use the chain of progenitors

identified in this way to reconstruct the mass evolution of a given halo back in time, down to the epoch of its first detection in the simulation.

About 10,000 halos (with maximum circular velocity $\gtrsim 120$ km/s, cf. Kravtsov et al. in this volume) can be identified at $z = 0$ in the analyzed $60 h^{-1}$ Mpc simulation box. Several hundreds of these halos are located in groups and clusters. This allows us to carry out for the first time a statistical comparison study of the clustering and mass evolution of isolated and satellite galaxy-size halos in an hierarchical cosmological model.

3 Results

We have identified halos using different input numerical parameters (size and number of particles) for the halo-finding algorithms. We find that for distances $\gtrsim 100 h^{-1}$ kpc the resulting halo-halo 2-point correlation function (CF) does not depend on these assumptions, as long as the number of particles in identified halo is $\gtrsim 30$. Note that the halo radius does not set limits on the inter-halo separation because halos are allowed to overlap. In Fig. 1 we present the halo-halo correlation function for halos with a maximum radius of $100 h^{-1}$ kpc and more than 28 particles ($3 \times 10^{10} h^{-1} M_{\odot}$). There is a statistically significant anti-bias on scales less than the correlation radius r_0 . The slope of the CF is ≈ -1.8 at scales $\approx 1 - 15 h^{-1}$ Mpc; at smaller scales the correlation function flattens slightly. In agreement with Colín et al. (1998) and results of many other studies, we find almost no time evolution of the CF at $z < 3$. The correlation function of DM, on the other hand, evolves rapidly which results in the strong evolution of bias and transition from $b > 1$ to $b < 1$ at small scales at $z \approx 1$ (see Fig. 2, see also Kravtsov et al. on the bias evolution in this volume).

The correlation function for the halos identified using our algorithms is compared in Fig. 1 to the CF of halos identified in a standard way using the FOF algorithm with linking radius corresponding to the virial overdensity. As we noted above, by definition the satellite halos are not present in the catalogs so gener-

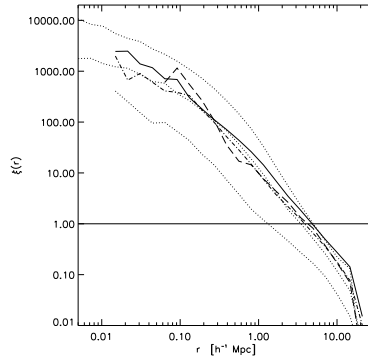


Figure 2. *The correlation function of halos with circular velocities $v_{circ} > 120$ km/s at $z = 0$ (solid line), $z = 1$ (dash-dotted line), and $z = 3$ (dashed line) in comparison to the correlation function of dark matter particles at the same redshifts (dotted lines; amplitude increases with decreasing redshift).*

ated. The comparison shows clearly that there are significant differences in both the slope and the amplitude at small ($\lesssim 7 h^{-1}$ Mpc) scales between these correlation functions. The higher amplitude of the CF determined using our halo-finding algorithms is explained by the larger number of small-separation halo pairs formed by satellite halos in groups and clusters missing in the FOF catalog. Note also that the CF of FOF halos does not extend down to $200 h^{-1}$ kpc due to the self-exclusion of halos at separations smaller than halo virial radii.

The mass of an object found by the HFOF algorithm *at virial overdensity* can be defined as the sum of linked particle masses. For all of the HFOF objects we identify the main progenitors at all epochs down to the halo formation time. To study the mass evolution due to merging and accretion we have divided these objects into four mass bins at $z = 0$: $M_0 > 5 \times 10^{12} M_{\odot}$ (bin 1), $5 \times 10^{12} M_{\odot} > M_0 > 5 \times 10^{11} M_{\odot}$ (bin 2), $5 \times 10^{11} M_{\odot} > M_0 > 5 \times 10^{10} M_{\odot}$ (bin 3), and $M_0 < 5 \times 10^{10} M_{\odot}$ (bin 4). Average mass evolution of halos in these bins normalized to the mass at $z = 0$ is shown in Fig. 3. We find a good agreement with the semi-analytical predictions (Lacey & Cole

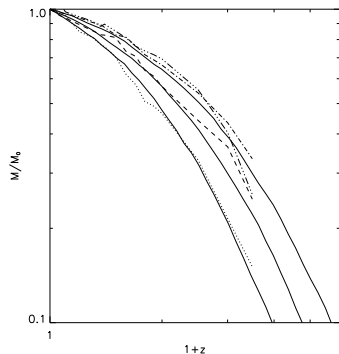


Figure 3. *Mass evolution of halos identified by the HFOF algorithm at virial overdensity. The dotted line is for average halo mass of $1.4 \times 10^{13} M_{\odot}$ (10 halos), the dashed for $1.1 \times 10^{12} M_{\odot}$ (20 halos), the dash-dotted for $7.7 \times 10^{10} M_{\odot}$ (417 halos) and the dash-triple-dotted line is for $2.1 \times 10^{10} M_{\odot}$ (82 halos). The solid lines show the predictions of semi-analytical model (kindly provided by Claudio Firmani) for 10^{13} , 10^{12} , and $10^{11} M_{\odot}$, from the bottom to the top.*

1993) for the evolution of these *isolated* halos.

Unfortunately, there is no simple and straightforward way to assign a mass for all halos identified in the simulation. Unlike the isolated halos identified by HFOF at virial overdensity, the satellite halos, although surviving, are subject to the tidal stripping which reduces their mass. They are limited therefore by tidal, rather than virial, radius. To assign masses to the halos we proceed as follows. The isolated halos are assigned the mass inside the virial radius or radius of $100h^{-1}$ kpc, whichever is smaller. The satellite halos are assigned the total mass of *gravitationally bound* particles within their tidal radius (or, again, within $100h^{-1}$ kpc, whichever is smaller). The tidal radius is determined as the radius at which the density profile of a halo flattens (stops decreasing).

We now construct the complete mass evolution histories for the set of *all* halos with the masses assigned as described above. We have divided these halos into five groups with

masses $M_0 > 10^{13} M_{\odot}$, $10^{13} M_{\odot} > M_0 > 5 \times 10^{12} M_{\odot}$, $5 \times 10^{12} M_{\odot} > M_0 > 10^{12} M_{\odot}$, $10^{12} M_{\odot} > M_0 > 5 \times 10^{11} M_{\odot}$, and $5 \times 10^{11} M_{\odot} > M_0$. We defined a subset of 3674 halos, mass of which increases (with allowance for small statistical fluctuations) at all epochs. As before, the mass of these objects is normalized to their final mass at $z = 0$. The mass evolution of these halos is shown in Fig. 4 (solid lines). The overall evolution is similar to the mass evolution of isolated halos described above (Fig. 3). Note, however, that while the mass evolution tracks are curved in Fig. 3, the mass evolution of the sample that includes satellites can be better represented by the straight lines in these log-log plots. This difference is due to the different halo selection procedure and to the different assignment of mass to the selected halos.

In the two lowest mass ranges we also find an additional subset of 2650 halos, whose masses decrease after $z = 1$ (dashed and dot-dashed curves in Fig. 4). Their mass increases at high redshifts, reaches a clear maximum and decreases thereafter. The mass of these halos grows first due to accretion of surrounding material and of smaller halos. At some point, however, these halos are being accreted by more massive halos and they start to loose mass due to the tidal stripping and interaction with other satellite halos. At $z = 1$ these halos are distributed similarly to the rest. At $z = 0$, however, they are clustered more strongly than the overall halo population.

This is illustrated in Fig. 5, which shows the correlation function for the two subsets of halos: always increasing mass and decreasing mass at $z < 1$. The correlation functions of the former has a lower amplitude and is not as steep as the correlation function of the latter. Note that the CF of the halos with the ever-increasing mass is anti-biased at scales $\lesssim 10h^{-1}$ Mpc, the CF of the halos that loose mass is actually positively biased. This reflects the fact that the loosing mass halos are found within massive systems such as massive galaxies, groups, and clusters, and are therefore strongly clustered.

One might speculate that this difference in the correlation functions may serve as a possible explana-

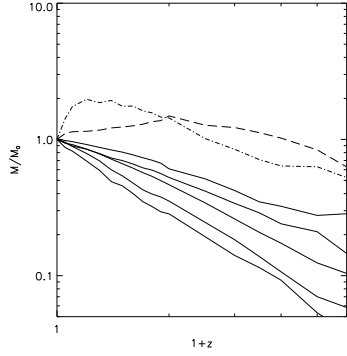


Figure 4. *Mass evolution of halos. The solid lines are for average masses of (from the bottom to the top) $1.2 \times 10^{13} M_{\odot}$ (14 halos), $6.6 \times 10^{12} M_{\odot}$ (34 halos), $1.9 \times 10^{12} M_{\odot}$ (442 halos), $7.0 \times 10^{11} M_{\odot}$ (534 halos), and $2.4 \times 10^{11} M_{\odot}$ (2650 halos). The dot-dashed (average mass of $6.9 \times 10^{11} M_{\odot}$) and the dashed (average mass of $2.0 \times 10^{11} M_{\odot}$) lines show the mass evolution of a subset of halos which loose mass between $z = 1$ and the present due to the tidal stripping in groups and clusters.*

tion for the color segregation of the correlation amplitude that has been recently observed (Carlberg et al. 1998). In fact, one could expect that the galaxies hosting halos which undergo different mass evolution also show different properties, and colors in particular. Further studies are necessary to test whether this simple picture can really explain the observations.

This work was funded by the NSF and NASA grants to NMSU. SG acknowledges support from Deutsche Akademie der Naturforscher Leopoldina with means of the Bundesministerium für Bildung und Forschung grant LPD 1996. We thank Claudio Firmani and Vladimir Avila-Reese for providing mass evolution predictions of semi-analytical models. The numerical simulations has been carried out at the Origin2000 computers at NCSA and Naval Research Laboratory (NRL).

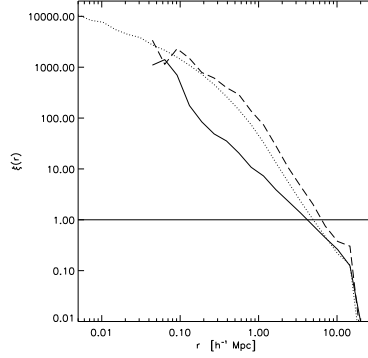


Figure 5. *The correlation function of halos with circular velocities $v_{\text{circ}} > 120$ km/s. The solid line corresponds to halos the mass of which always increases (solid lines in Fig. 4), the dashed line corresponds to halos which loose mass during evolution (dashed and dashed-dotted lines in Fig. 4). The correlation function of dark matter particles is shown by the dotted line.*

Carlberg R.G. et al., 1997, Phil.Trans.R.Soc.Lond.A (astro-ph/9805131)

Colín P., Klypin A.A., Kravtsov A.V., Khokhlov A.M., 1998, ApJ submitted (astro-ph/9809202)

Ghigna S., et al., 1998, MNRAS 300, 146

Klypin A.A., Gottlöber S., Kravtsov A.V., Khokhlov A.M., 1998, ApJ submitted (astro-ph/9708191) (KGKK)

Kravtsov A.V., Klypin A.A., Khokhlov A.M., 1997, ApJS, 111, 73

Moore B., Katz N., Lake G., 1996, ApJ, 457, 455

Lacey, C., Cole, S. 1993, MNRAS, 262, 627